

# The influence of gamma irradiation and aging on degradation mechanisms of ultra-high molecular weight polyethylene

F. J. BUCHANAN

*School of Mechanical and Manufacturing Engineering, The Queen's University of Belfast, Belfast, N. Ireland, BT9 5AH, UK*

J. R. WHITE

*Materials Division, Dept. of Mechanical, Materials and Manufacturing Engineering, University of Newcastle, Newcastle upon Tyne, NE1 7RU, UK*

B. SIM, S. DOWNES

*School of Biomedical Sciences, Medical School, University of Nottingham, Nottingham, NG7 2UH, UK*

*E-mail: f.buchanan@QUB.ac.uk*

The aging behavior of ultra-high molecular weight polyethylene (UHMWPE) has been studied following gamma irradiation in air. Accelerated aging procedures used elevated temperature (70 °C), pressurized oxygen (5 bar) and applied stress. Shelf and *in vivo* aged components have also been investigated. The variation in polymer properties with depth into the polymer was determined using density measurements, infra-red spectroscopy and differential scanning calorimetry. Accelerated aging in pressurized oxygen resulted in peaks in polymer density and degree of oxidation up to 500 μm below the polymer surface. Shelf and *in vivo* aging was also found to result in increased density at or below the component surfaces. Changes in density were mainly due to changes in crystallinity within the UHMWPE and, to a smaller extent, due to oxygen incorporation within the polymer. The application of stress did not appear to influence the accelerated aging of UHMWPE.

A method for estimating the residual stress distribution in the UHMWPE using the measured changes in density is proposed. This study has indicated that oxidation of UHMWPE may lead to the development of tensile residual stresses, near the component surface, in the region of 1.7 MPa. These stresses may contribute to the failure mechanism of UHMWPE acetabular cups or knee tibial trays during service.

© 2001 Kluwer Academic Publishers

## 1. Introduction

Ultra-high molecular weight polyethylene (UHMWPE) has been the material of choice for the wear surface (against a metallic or ceramic counterface) of total joint replacements for the past three decades [1]. The life of these components is considered to be related to the wear performance of the UHMWPE used and the method of sterilization [2–5]. Gamma irradiation has been the most common method of sterilization but results in the formation of free-radicals, rendering the UHMWPE unstable. Oxygen can diffuse into the polymer over time, reacting with the free-radicals present and causing chain scission (a reduction in polymer molecular weight). This is accompanied by internal cross-linking reactions, with the overall result being changes in physical properties of the polymer which influence wear performance [6]. Generally chain scission is

considered to be detrimental to wear performance whereas cross-linking is thought to be beneficial. A high wear rate results in a high generation of wear debris. This enters the bone-joint interface and produces an inflammatory response. This has been linked to bone lysis which leads to loosening of the component itself (aseptic loosening) [7]. Revision surgery is normally the only option at this stage, but this is a costly and inconvenient operation.

Several accelerated aging techniques have been used to study the mechanisms of UHMWPE degradation [8–10]. The current work uses a pressurized oxygen “bomb” to age polymers under conditions of elevated oxygen pressure and temperature. Comparisons have been made with retrieved (*in vivo*) and shelf aged components. This work also includes a study on the influence of applied stress on accelerated aging of

TABLE I Details of shelf and *in vivo* aged components

Description	Sterilization procedure	Material	Shelf aging time	<i>In vivo</i> aging time
Acetabular cup	Gamma, air, 25–40 kGy	GUR412	4 years	0
Acetabular cup	Gamma, air, 25–40 kGy	Chirulen block	1 month	5 years
Acetabular cup	Gamma, air, 25–40 kGy	Chirulen block	1 year	5 years

UHMWPE. Examination and characterization of gamma irradiated UHMWPE samples, before and after exposure to accelerated aging processes involves use of differential scanning calorimetry (DSC), Fourier transform infra-red spectroscopy (FTIR) and density measurements. A method for estimating residual stress distributions in the UHMWPE following gamma irradiation and aging is proposed.

## 2. Experimental

### 2.1. Materials

UHMWPE material was supplied by Perplas Medical Ltd (Todmoden, Lancs., UK) in the form compression molded blocks of thickness 55 mm, produced from powder grade GUR1050 UHMWPE.

The compression molded block was initially reduced in size by band sawing. Machining to final specimen dimensions (rectangular blocks  $60 \times 15 \times 10$  mm or sheets of 2 mm thickness) was performed using a milling machine fitted with a single-point fly cutter, run at approximately 500 rpm. This technique has been successfully employed by White [11] who reported it not to cause melting or machining damage to the polymer. Double-sided adhesive tape was used to hold the specimens in place during the milling process. Shelf and *in vivo* aged components are described in Table I.

### 2.2. Sterilization and aging procedures

Test specimens were gamma sterilized in air at standard sterilization doses of 25 and 40 kGy (Isotron Ltd, Swindon, UK). The samples were stored at  $-20^\circ\text{C}$  (one week after irradiation) until analysis could be performed.

Accelerated aging of UHMWPE specimens under pressurized oxygen conditions was carried out using an ‘‘oxygen bomb’’. All specimens were removed from their packaging prior to aging by this method. The pressurized bomb (manufactured from aluminum) had internal dimensions of 200 mm height by 250 mm diameter and wall thickness 20 mm. Specimens were stacked in the bomb using steel mesh spacers to ensure that no specimens contacted the sides of the bomb or each other. Parameters for oxygen aging were a pressure of 5 bar oxygen and a temperature of  $70^\circ\text{C}$  [9]. Time periods of 4 and 8 days were used (abbreviated to O4 and O8 respectively).

Tests were also performed using a three-point bend rig, placed within the oxygen bomb (Fig. 1). A 2 kg load was hung from the center of a UHMWPE bar (dimensions  $120 \times 15 \times 10$  mm). Using Equation 1 the surface flexural stress was calculated to be 2 MPa at the midpoint. This

would be tensile at the lower surface and compressive at the upper surface.

$$\sigma_f = \frac{3LF}{2bh^2} \quad (1)$$

where  $\sigma_f$  = surface flexural stress at midpoint,  $L$  = distance between end supports,  $F$  = load at midpoint,  $b$  = specimen width,  $h$  = specimen height. These applied stress levels are similar in value to maximum levels predicted for residual stress development.

### 2.3. Characterization methods

#### 2.3.1. Sample preparation for density measurement, FTIR and DSC

Test samples were obtained from irradiated and aged specimens by core drilling perpendicular to the  $60 \times 15$  mm face to obtain cylinders 6 mm in diameter by 10 mm in length (Fig. 2). The drilling operation was performed no closer than 7.5 mm from the specimen edges. The cylinders were then microtomed to obtain disks of 200  $\mu\text{m}$  thickness by 6 mm diameter. For each cylindrical specimen 24 disks were obtained, i.e. providing a depth profile up to 4800  $\mu\text{m}$  (approximately 5 mm) from the specimen surface.

#### 2.3.2. Density measurement

Depth profiles of density were obtained using a density gradient column. The column was filled with an ethanol-water mixture to give a density range of  $0.93$  to  $0.96 \text{ g cm}^{-3}$ . Before filling the ethanol-water mixtures were degassed in vacuum to prevent the formation of air bubbles during use. Eight glass density floats were used to calibrate the column which was maintained at a temperature of  $23 \pm 1^\circ\text{C}$  during measurement. For samples which did not display a variation in density with depth the results were statistically compared using a single-tailed  $t$  procedure for equal variances.

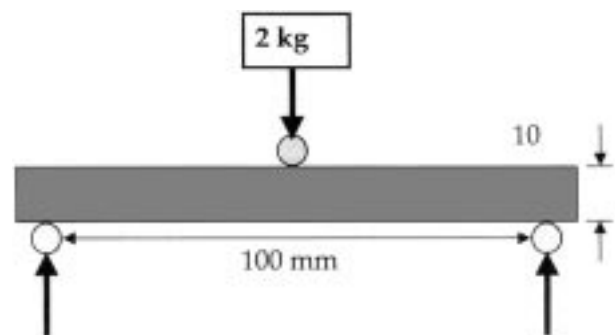


Figure 1 Configuration of three-point bend rig, used to apply static loads during accelerated aging.

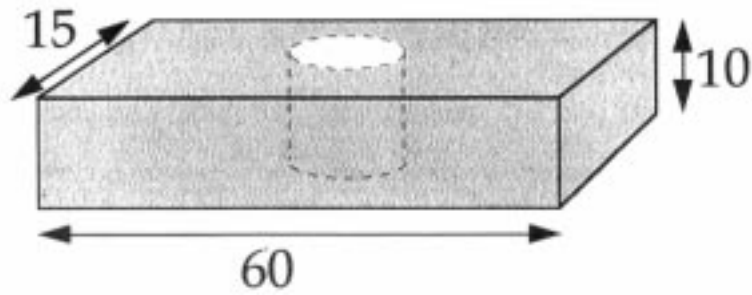


Figure 2 UHMWPE specimen showing location of core drilled sample (dimensions in mm).

### 2.3.3. Infra-red spectroscopy

FTIR was used for measurement of the extent of oxidation within the polymer. A Perkin Elmer 2000 FTIR with i-series microscope was used for all measurements. Spectra were obtained for each 200  $\mu\text{m}$  polymer disk in the range 4000 to 750  $\text{cm}^{-1}$ , in transmission mode. The peak height in absorbance at 1717  $\text{cm}^{-1}$  (associated with the C = O keto-carbonyl groups in the polyethylene) was measured along with the peak height in absorbance at 2022  $\text{cm}^{-1}$  (polyethylene reference peak,  $-\text{CH}_2-$  vibration in both the crystalline and amorphous regions). The ratio between these two peaks was calculated to give an “oxidation index” [12].

### 2.3.4. Differential scanning calorimetry

A Perkin Elmer model DSC7 was used to determine the degree of crystallinity of the polymer. The test procedure used a 10  $^{\circ}\text{C}/\text{min}$  heating rate over a temperature range of 30  $^{\circ}\text{C}$  to 160  $^{\circ}\text{C}$ . The degree of crystallinity was estimated using a value of 289.74 J/g for fully crystalline polyethylene [13].

## 2.4. Analysis

### 2.4.1. Residual stress distribution

Consider a mass of material that undergoes a volume change from  $V_1$  to  $V_2$  and a corresponding density change from  $\rho_1$  to  $\rho_2$ . If the volume strain is isotropic then the linear strain,  $\epsilon$ , is given by:

$$\frac{V_1 - V_2}{V_1} = \frac{\rho_2 - \rho_1}{\rho_2} = 3\epsilon \quad (2)$$

If the volumetric change is confined to a relatively thin layer on top of a massive substrate then the shrinkage is resisted and the residual stress so generated is equibiaxial and is given by:

$$\sigma_i = \frac{E\epsilon}{1 - \nu} = \frac{E}{1 - \nu} \frac{\rho_2 - \rho_1}{3\rho_2} \quad (3)$$

where  $E$  is the Young’s Modulus and  $\nu$  is Poisson’s ratio. The choice of value for  $E$  requires careful consideration. UHMWPE displays considerable stress relaxation therefore the relaxation modulus at long times has been applied. This is because the timescale of the application of interest here is measured in years. The value of the Young’s modulus chosen for the calculations presented here is deduced for the data and model given by Waldman and Bryman [14] and is taken to be 210 MPa. Poisson’s ratio,  $\nu$ , has been taken as 0.41 [15]. Since

residual stress changes should be based on relative changes in density at different locations within the UHMWPE specimens the value used for  $\rho_1$  in Equation 3 was taken as the minimum density value for each specimen.

### 2.4.2. Fractional crystallinity

Although the calculations of residual stress are made directly from the density data it is of interest to determine changes in the fractional crystallinity,  $f_c$ , that take place. This is because the density can be affected by changes additional to the changes in crystallinity and the volumetric behavior upon which the residual stress calculation is based may not be as simple as assumed above. Fractional crystallinity values have been calculated from the density data using the assumption that the samples consist of two phases: a crystal phase with a density of 0.998  $\text{gcm}^{-3}$  and a non-crystalline phase with a density of 0.854  $\text{gcm}^{-3}$ . The fractional crystallinity,  $f_c$ , (on a mass basis) for a sample of UHMWPE with a density,  $\rho$ , is then given by:

$$f_c = \frac{998(\rho - 0.854)}{144\rho} \quad (4)$$

## 3. Results

### 3.1. Density measurement

#### 3.1.1. Unaged UHMWPE

The average density (for depths of 0 to 5 mm) of unaged UHMWPE samples following gamma irradiation is shown in Fig. 3 (five samples per treatment). The density was found to increase significantly ( $p < 0.01$ ) for as-

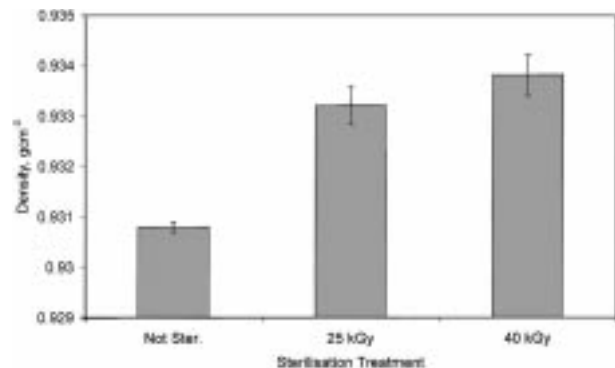


Figure 3 Average density measurements for UHMWPE following gamma irradiation.

irradiated samples. Density also tended to increase with irradiation dose ( $p < 0.05$ ).

### 3.1.2. Accelerated aging of UHMWPE

UHMWPE specimens were subjected to accelerated aging conditions of 4 to 8 days in pressurized oxygen ( $70^\circ\text{C}$ , 5 bar, *O4* and *O8* respectively). The gamma irradiated specimens all showed significant variation in density after aging. For the *O4* age the density was found to be highest at the surface and decrease for depths up to 5 mm into the specimen (Fig. 4). For the *O8* age the peak in density was observed approximately 500  $\mu\text{m}$  below the specimen. The average density increase occurring between 4 and 8 days aging was also found to be approximately two fold greater than the average density increase for between 0 and 4 days aging.

Fig. 5 shows typical infra-red spectra obtained at various depths through the gamma irradiated and aged UHMWPE. The oxidation ratio was obtained by dividing the peak height at  $1717\text{ cm}^{-1}$  by the peak height at  $2022\text{ cm}^{-1}$ .

Fig. 6 shows a comparison of oxidation index depth profiles for UHMWPE specimens gamma irradiated at 25 and 40 kGy and subjected to accelerated aging. These show similar trends to the results of density measurements.

UHMWPE specimens (gamma irradiated, 25 kGy) were also aged for 8 days ( $70^\circ\text{C}$ , 5 bar) under conditions of applied stress. Depth profiles were obtained either at the specimen midpoint (maximum flexural stress) or at the position of the end supports (zero flexural stress). The

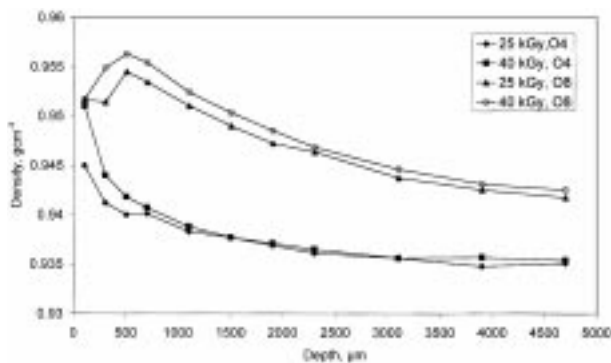


Figure 4 Density depth profiles for UHMWPE gamma irradiated at 25 and 40 kGy and aged under accelerated conditions (*O4*, *O8*).

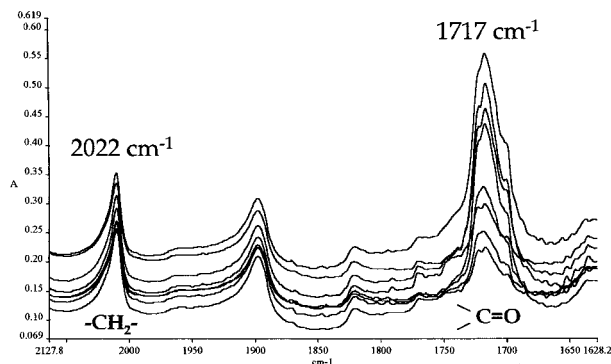


Figure 5 Typical infra-red absorption spectra for gamma irradiated and aged UHMWPE (25 kGy, *O8*, 200–4800  $\mu\text{m}$ ).

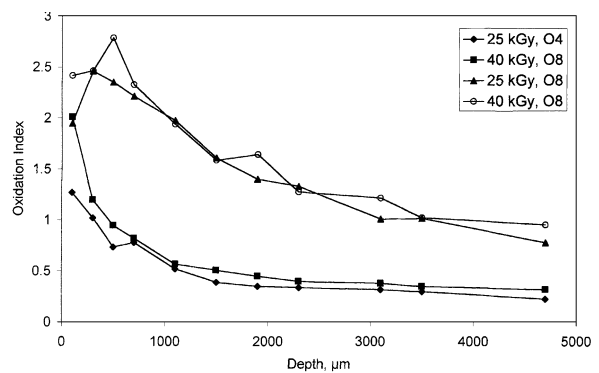


Figure 6 FTIR oxidation index depth profiles for UHMWPE gamma irradiated at 25 and 40 kGy and aged under accelerated conditions (*O4*, *O8*).

depth profiles were analyzed by both density measurement and FTIR starting at either the upper (compressive) surface or the lower (tensile) surface. Results for both density measurement and FTIR indicated that there was no significant difference in density or oxidation ratio between these various depth profiles (Figs 7 and 8).

### 3.1.3. Shelf and in vivo aging of UHMWPE

Density depth profiles for shelf and *in vivo* aged components are shown in Fig. 9. For shelf aged components maximum density occurred between 1 and 2 mm below both the inner (concave) and outer (convex) surfaces. For typical *in vivo* aged components maximum density occurred either on or 0.5 mm below the inner

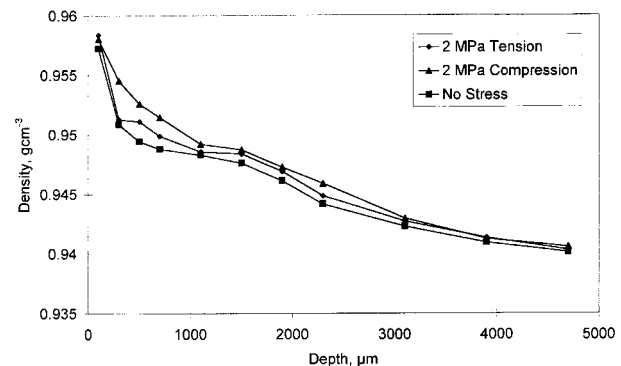


Figure 7 Density depth profiles for UHMWPE gamma irradiated at 25 kGy and aged under applied stress (*O8*).

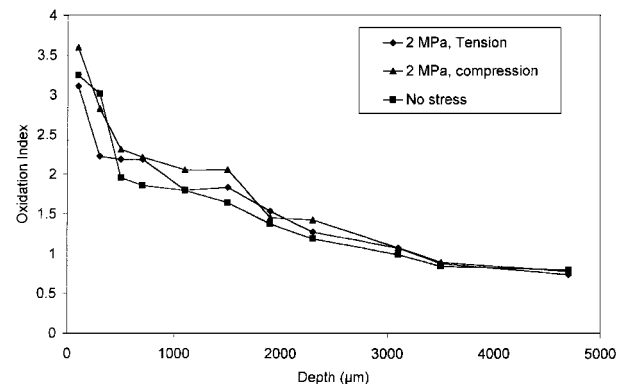


Figure 8 FTIR oxidation index depth profiles for UHMWPE gamma irradiated at 25 kGy and aged under applied stress (*O8*).

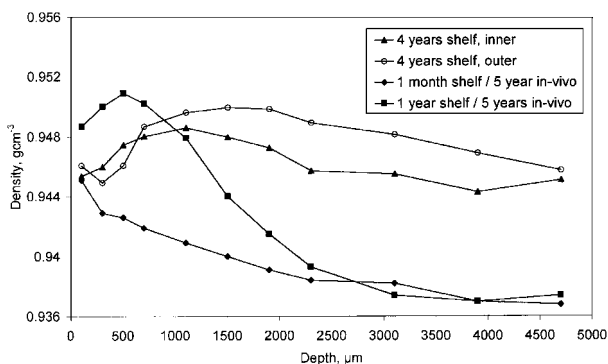


Figure 9 Density depth profiles for shelf and *in vivo* aged UHMWPE.

(concave) surface. It should be noted that *in vivo* components are likely to have experienced some wear on this surface. This would influence depth profiles.

### 3.2. Weight change due to accelerated aging

Unsterilized and gamma irradiated (25 kGy) specimens were aged in the oxygen bomb for 8 day time periods (O8). Weight gains were recorded for unsterilized and gamma irradiated UHMWPE. The ratio between these two weight gains was found to have a similar value to that for the ratio between average density changes for the same treatments (Table II).

Using results for polymer weight gain, values were calculated for the effect of absorbed oxygen on the density of UHMWPE. This was achieved using the oxidation index depth profile for gamma irradiated UHMWPE aged for 8 days in the oxygen bomb (O8). This assumes the weight gain to be related to oxygen incorporation in the polymer and therefore the carbonyl peak height at  $1717\text{ cm}^{-1}$ . Fig. 10 shows the calculated

TABLE II Average weight and density changes for unsterilized and gamma irradiated UHMWPE following accelerated aging (O8)

	A. Unsterilized, aged (O8)	B. Sterilized 25 kGy, aged (O8)	Ratio (A/B)
Weight change (%)	0.07	0.31	0.22
Density change ( $\text{g}/\text{cm}^3$ )	0.0036	0.0154	0.23

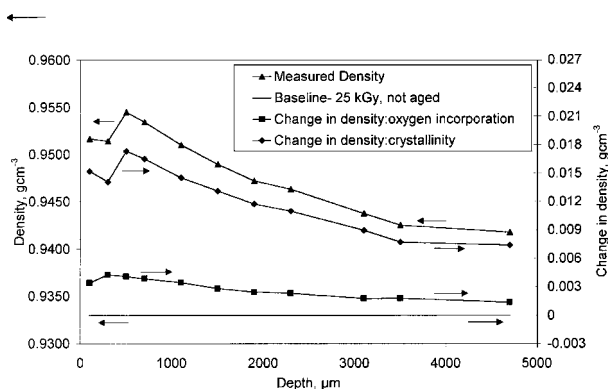


Figure 10 Density depth profile of UHMWPE (25 kGy, O8), showing contribution from oxygen incorporation (weight change) and fractional crystallinity change.

density change due to oxygen incorporation, assuming this to have no significant influence on volume. This was compared to the total measured density change and shows the influence of oxygen incorporation in the polymer on the total density change. It is assumed that total density increase is a combination of increased crystallinity and oxygen incorporation.

### 3.3. Fractional crystallinity

Values obtained from Equation 4 for fractional crystallinity and experimental values, obtained by DSC, are compared in Fig. 11 for accelerated aged UHMWPE (25 kGy, O8). Also shown in this figure are the corrected values of fractional crystallinity, where results have been adjusted to account for the effects of density change due to oxygen incorporation (no volume change). Fig. 12 shows the correlation between fractional crystallinity obtained from density results and values for DSC.

### 3.4. Residual stress distribution

Predicted values for residual stress distributions, using Equation 3, are shown in Fig. 13 for accelerated aging procedures and in Fig. 14 for shelf and *in vivo* aged specimens. Using a value for Young's modulus of 210 MPa a maximum value of residual stress was calculated to be 1.9 MPa for accelerated aged UHMWPE (O4) and 1.7 MPa for retrieved components (1 year shelf/1 year *in vivo*).

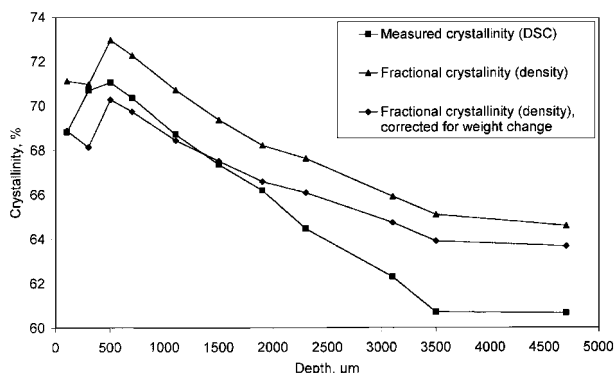


Figure 11 Crystallinity measured by DSC for UHMWPE (25 kGy, O8), compared to fractional crystallinity calculated for density values.

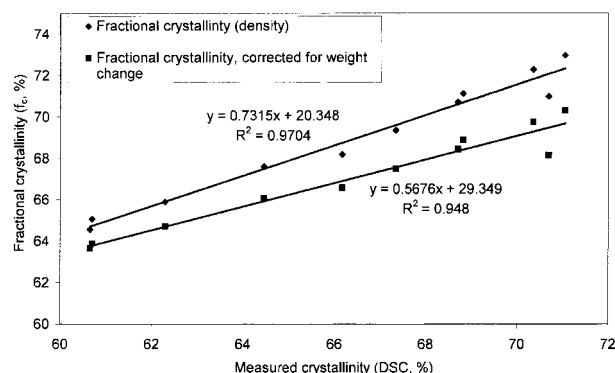


Figure 12 Correlation between crystallinity measured by DSC and fractional crystallinity predicted from density values for UHMWPE (25 kGy, O8).

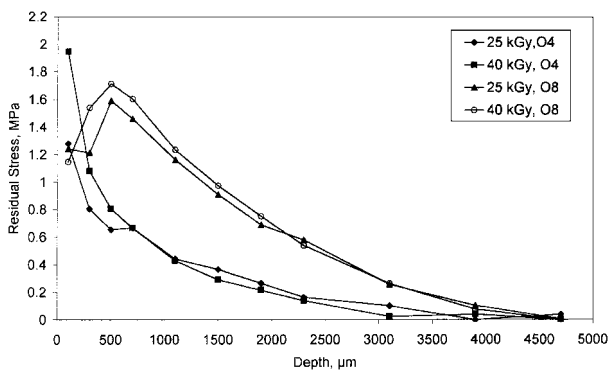


Figure 13 Residual stress distribution predicted for UHMWPE gamma irradiated at 25 and 40 kGy and aged under accelerated conditions (O4, O8).

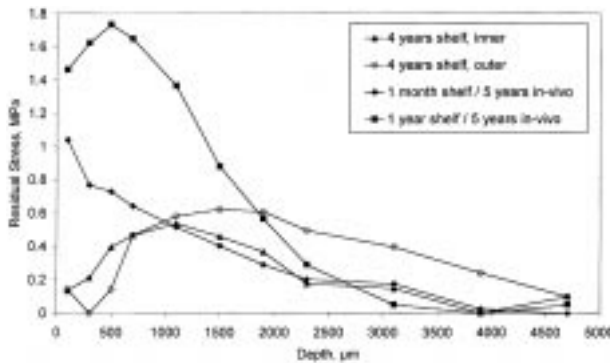


Figure 14 Residual stress distribution predicted for shelf and *in vivo* aged UHMWPE.

## 4. Discussion

### 4.1. Unaged UHMWPE

The effects of sterilization treatments by gamma irradiation caused significant increases in density of the UHMWPE. The increased density caused by gamma irradiation would seem to correlate with increased crystallinity (crystalline polyethylene being of higher density than the amorphous phase) and probably arises from chain scission caused by the irradiation process lowering the molecular weight of the polymer [16]. The increased freedom of movement of the entangled, amorphous polymer chains enables rearrangement into a lower energy, crystalline state. Oxygen will react with free-radicals in the polymer causing further chain scission. Rimnac *et al.* [2] found the density of UHMWPE to increase from approximately  $0.9335$  to  $0.936 \text{ g cm}^{-3}$  following gamma irradiation in air. This is in good agreement with changes observed in the current results, although the initial sample density differs.

### 4.2. Accelerated aging of gamma irradiated UHMWPE

Depth profiles for density, oxidation ratio and crystallinity showed good correlation for all accelerated aging treatments. For the O4 aging treatment the peaks in these properties generally occurred at the specimen surface. For aging in pressured oxygen for 8 days (O8) the peaks generally occurred up to  $500 \mu\text{m}$  below the specimen

surface. The oxidation process is considered to be a diffusion-controlled phenomenon explaining the decrease in oxidation with depth and the increased rate of oxidation for aging in pressured oxygen. This does not, however, account for the peak in oxidation below the specimen surface for 8 days aging in pressurized oxygen. Perhaps the most convincing explanation for the formation of subsurface maximum in oxidation comes from the work of Yeom *et al.* [6], who describe the cascade of events occurring at various depths within gamma irradiated UHMWPE. At the surface of the UHMWPE the  $\text{O}_2$  concentration is highest and most primary alkyl radicals ( $-\text{CH}_2 \cdot \text{CH}_2-$ ) and secondary alkyl radicals ( $-\text{CH}_2-\text{CH} \cdot-$ ) produced by gamma irradiation will react to form peroxy radicals ( $-\text{CH}-\text{O}-\text{O} \cdot$  or  $> \text{CH}-\text{O}-\text{O} \cdot$ , respectively). Other secondary alkyl radicals can combine to form cross-links. A large concentration of peroxy radicals exists at the surface and these can combine to form ketones, a reaction which does not produce any further free radicals i.e. the end of the cascade. In the subsurface region, on the other hand, fewer peroxy radicals form, due to the lower  $\text{O}_2$  concentration in this region. Because these peroxy radicals will be further apart there will be less tendency to react with each other and more tendency to abstract H atoms from the polyethylene chains, thereby forming hydroperoxides and new free radicals. This initiates a cascade of reactions which forms carbonyl groups, chain scission and further free radicals. As oxygen diffuses into the UHMWPE, further reaction with the newly created free radicals can occur, eventually leading to higher levels of oxidation in this subsurface region compare with the surface. Deeper into the UHMWPE there will be less oxygen available for reaction so most of the radicals will combine to produce cross-links.

The average density increase between 4 and 8 days aging was also found to be approximately two fold greater than the average density increase between 0 and 4 days aging. Similar trends were observed for changes in oxidation ratio. It would appear that the oxidation rate is initially low and accelerates between 4 and 8 days aging. This observation may relate to the findings of Currier *et al.* [17] for shelf aged components. They observed that the oxidation rate of UHMWPE tibial bearings, gamma sterilized in air, was relatively low during the first five years of shelf life, but increased by an order of magnitude after five years shelf life. This auto-acceleration phenomenon is considered to be in part due to the cascade of free-radical reactions, as described by Yeom *et al.* [6] and in part due to changes in the diffusion rate of oxygen through the UHMWPE as it degrades. A quantitative protocol, based on oxygen permeability has been developed by Yau *et al.* [18] to evaluate particle consolidation in UHMWPE. A higher oxygen permeability indicates that oxygen can enter the material more readily, thereby causing greater oxidation in the presence of free radicals. They measured significant variations in oxygen permeability depending on resin type and processing route. Other workers [19] have shown that diffusion of oxygen occurs preferentially along grain boundaries and into the grains through the amorphous regions of the polymer. Grain boundaries may be present

where incomplete consolidation of the original resin particles has occurred [20]. Changes in crystallinity of the polymer, resulting in residual tensile stresses, may also influence oxygen permeability. Assuming the overall volume to remain constant (due to the constraining effect of the bulk underlying material) and oxygen diffusion to occur mainly in the amorphous regions of the UHMWPE, as these amorphous regions crystallize the remaining amorphous phase may decrease in density. This means that this remaining amorphous polymer structure, between crystalline regions, will become more ‘open’, allowing easier ingress of the oxygen molecules (Fig. 15). Goldman *et al.* [21] examined the morphology of UHMWPE using transmission electron microscopy (TEM) and found that gamma irradiated UHMWPE (aged for 10 months) had a more ordered, lamellae structure than the non-irradiated material, suggesting an increase in crystallinity. In fractional crystallinity calculations the density of amorphous UHMWPE (between crystalline lamellae) was assumed to be constant ( $0.854 \text{ g/cm}^3$ ). This assumption may be incorrect and account for the correlation between crystallinity measured by DSC and fractional crystallinity having a gradient of less than one (Fig. 10). The gradient of this correlation can be forced to equal one if the density of amorphous UHMWPE is assumed to decrease as the polymer crystallinity increases. For example a gradient of one would be obtained if the density of amorphous UHMWPE decreased from  $0.854 \text{ g/cm}^3$  to  $0.837 \text{ g/cm}^3$  as the crystallinity (measured by DSC) increased from 61% to 71%.

The application of either tensile or compressive stress to the UHMWPE during accelerated aging had no significant effect on the rate or profile of oxidation (applied stress levels were of the same order as levels predicted for residual stress development). Although mechanico-oxidative degradation of polymers is a recognized phenomenon [22] it seems that, in the current work, this level of applied stress has not influenced the rate of degradation.

### 4.3. Shelf and *in-vivo* aging

Kurtz *et al.* [23] have measured density changes for shelf stored and *in vivo* components for up to 44 months of aging. Their findings indicate that average density increases in a linear manner with aging time over this time period and maximum density occurs 1–2 mm below the component surface. The rate of average density change was found to be  $1.86 \times 10^{-4} \text{ g/cm}^3/\text{month}$ . The current results for shelf aging show maximum densities to occur 1–2 mm below the component surfaces (in this case for 48 months of shelf aging). This is in good agreement with the findings of Kurtz *et al.* [23]. If a linear density increase is assumed and an initial density of  $0.935 \text{ gcm}^{-3}$  then the rate of average density change, for the current work, is calculated to be  $2.18 \times 10^{-4} \text{ g/cm}^3/\text{month}$ .

Density depths profiles were obtained starting from either the inner (concave) and outer (convex) surface of the acetabular cup. Differences in these profiles suggests component geometry may influence the results. Oxygen diffusing into the concave side of the cup will tend to dilute with depth and *vice versa* on the convex side.

### 4.4. Residual stress distribution

Predicted residual stress distributions were of a similar order for both accelerated and real aging of UHMWPE. This indicated that accelerated aging would seem to be a valid method for simulating density changes which occur in real aged components. Due to the temperature of accelerated aging ( $70^\circ\text{C}$ ) it should be emphasized that actual residual stress distributions would differ from those predicted, due to stress relaxation at this temperature. However, the values of density are valid and can be used as a tool to predict residual stresses which may occur in real components.

It is important to note that residual stress determinations were based on relative density changes. Although density changes were high for the O8 treatment and shelf aging (assuming an original density of between 0.93 and  $0.935 \text{ gcm}^{-3}$ ) the maximum residual stresses were, in

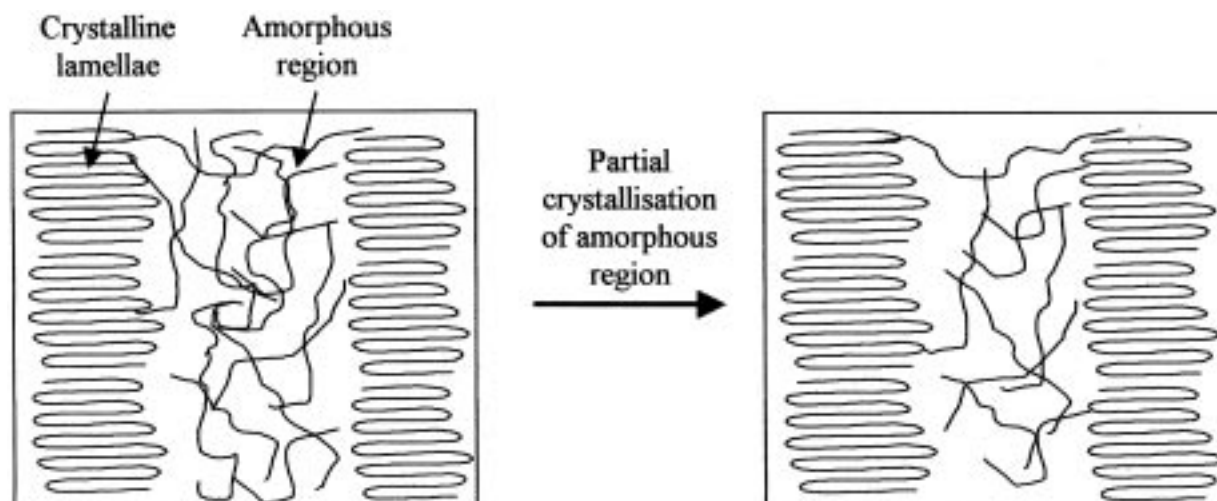


Figure 15 Schematic representation of UHMWPE crystallization, resulting in a more ‘open’ amorphous region.

some cases, lower than those for the *O4* treatment or *in vivo* aging, respectively. It would seem that as degradation of the UHMWPE proceeds oxygen can diffuse further into the polymer, thus reducing differences between surface and interior densities.

The residual stress distributions have been determined using a value of Young's modulus of 210 MPa. This has been based on the relaxation modulus at long times at 37°C and deduced for the data and model given by Waldman and Bryman [14]. Kurtz *et al.* [24] have measured the Young's modulus relative to density changes in UHMWPE, in this case using a rate of 3 mm/min. They found values increased from 1.1 GPa to 1.7 GPa with increasing density for densities in the range 0.937 to 0.958 gcm<sup>-3</sup>. These values are one order of magnitude higher than those of Waldman and Bryman [14] and indicate the significant effect of stress relaxation on modulus of UHMWPE.

Residual stresses produced near the component surface are tensile and relaxation is likely to occur over long time periods. Stress relaxation, like creep, is very temperature dependent and therefore may have a stronger effect in implanted components (37°C) than for shelf aged components ( $\approx 20^\circ\text{C}$ ). Lee and Pienkowski [25] have measured compressive creep of UHMWPE at 37°C. They found that approximately 85% of the total creep occurred in the first 16 h of a one week test and the total creep was linearly related (30.8  $\mu\text{m}/\text{MPa}$ ) to the applied pressure. It should be emphasized that actual residual stresses may differ from predicted values depending on how quickly stress relaxation occurs following the crystallinity changes. For example, more rapid surface crystallinity changes (relative to the bulk polymer) may lead to development of higher residual stresses than predicted. However, over long time periods, stress relaxation is likely to be significant, resulting in lower residual stresses than predicted.

It is important to consider whether the residual stress in UHMWPE acetabular cups is likely to have a bearing on the overall wear resistance, or failure mechanism of the component. Other workers [26] have reported radial cracks to be present in acetabular components following less than 10 years *in vivo*. These radial cracks occurred in the region of maximum crystallinity (68%). It seems that any residual tensile stresses present would contribute to the formation of these cracks. As oxidation proceeds the tensile strength and elongation to break of UHMWPE decrease [27]. Residual stresses will be highest in the region of maximum crystallinity and tensile strength will be lowest. At some point the cumulative effect of applied and residual stresses may exceed the tensile strength, resulting in the formation of these radial cracks.

## 5. Conclusions

Accelerated aging at 70°C for up to 8 days in pressured oxygen appears to be an effective method of aging UHMWPE and can be related to degradation of real components. Characterization by density measurement, infra-red spectroscopy and differential scanning calorimetry all indicated similar trends in properties with depth below the specimen surface. Changes in density were mainly due to changes in crystallinity within the

UHMWPE and, to a smaller extent, due to oxygen incorporation within the polymer. The rate of UHMWPE oxidation increases with accelerated aging time. This is considered to be due to a cascade of free-radical reactions occurring within the polymer and changes in the diffusion rate of oxygen as the polymer degrades. The rate of oxidation does not appear to be influenced by the application of stress (up to 2 MPa) during the accelerated aging process.

This study has indicated that oxidation of UHMWPE, following gamma irradiation, may result in tensile residual stress on or below the component surface. The value of this stress is predicted to be in the region of 1.7 MPa. This may contribute to the failure mechanism of UHMWPE acetabular cups or knee tibial trays during service.

## Acknowledgments

This work has been supported by the Department of Trade and Industry under the Characterization of Advanced Materials (CAM) program. Materials have been supplied by Perplas Medical Ltd.

## References

1. C. M. AGRAWAL, D. M. MICALLEF and J. MABREY, in "Encyclopedic Handbook of Biomaterials and Bioengineering, Part A: Materials", edited by D.L. Wise, (Marcel Dekker Inc., New York, Basel, Hong Kong, 1995) p. 1759.
2. C. M. RIMNAC, R. W. KLIEN, F. BETTS and T. M. WRIGHT, *J. Bone Joint Surg.* **76-A** (1994) 1052.
3. H. WITKIEWICZ, M. DENG, T. VIDOVSZKY, M. E. BOLANDER and M. G. ROCK, *J. Biomed. Mater. Res.* **33** (1996) 73.
4. M. CHOUDHURY and I. M. HUTCHINGS, *Wear* **203-204** (1997) 335.
5. J. FISHER, E. A. REEVES, G. H. ISAAC, K. A. SAUM and W. M. SANFORD, *J. Mater. Sci.: Mater. Med.* **8** (1997) 375.
6. B. YEOM, Y.-J. YU, H. A. MCKELLOP and R. SALOVEY, *J. Polym. Sci. Polym. Chem.* **36** (1998) 329.
7. C. HARLAN, M. D. AMSTUTZ, P. CAMPBELL, M. D. KOSSOVSKY and I. C. CLARKE, *Clin. Orthop. Related Res.* **276** (1992) 7.
8. D. C. SUN, C. STARK and J. H. DUMBLETON, in "ACS Symposium Series, Irradiation of Polymers", (American Chemical Society, 1996) pp. 340-349.
9. W. M. SANFORD and K. A. SAUM, in "41st Annual Meeting, Orthopaedic Research Society", 13-16 February, 1995. (Orlando, Florida: The Orthopaedic Research Society), 119.
10. B. D. FURMAN, J. LELAS, H. WALSH, S. SODHA, D. McNULTY, T. SMITH and S. L. I., in "24th Annual Meeting of the Society for Biomaterials", 22-26 April, 1998 (San Diego, CA: Society for Biomaterials).
11. J. R. WHITE, *Polymer Testing* **4** (1984) 165.
12. H. A. MCKELLOP, F. W. SHEN, Y. J. YU, B. LU, R. SALOVEY and P. CAMPBELL, in "Polyethylene Wear in Orthopaedic Implants Workshop", 30 April-4 May, 1997 (Society for Biomaterials, New Orleans, Louisiana) 20.
13. R. S. PASCAUD, W. T. EVANS, P. J. J. MCCULLAGH and D. FITZPATRICK, *J. Biomed. Mater. Res.* **32** (1996) 619.
14. S. D. WALDMAN and J. T. BRYMAN, *J. Appl. Biomater.* **5** (1994) 333.
15. C. M. RIMNAC, T. H. BALDINI, T. M. WRIGHT, K. A. SAUM and W. M. SANFORD, in "42nd Annual Meeting, Orthopaedic Research Society", 19-22 February, 1996. Atlanta, Georgia, p. 481.
16. V. PREMNATH and W. H. HARRIS, *Biomater.* **17** (1996) 1741.
17. B. H. CURRIER, J. H. CURRIER, D. E. COLLIER, M. B.



- MAYOR and R. D. SCOTT, *Clin. Orthop. Related Res.* **342** (1997) 111.
18. S. S. YAU, B. EDWARDS, D. C. SUN, C. STARK and J. H. DUMBLETON, in "24th Annual Meeting of the Society for Biomaterials", 22–26 April, 1998, San Diego, CA, p. 501.
  19. O. K. MURATOGLU, C. R. BRADGON, M. JASTY and W. H. HARRIS, in "Fifth World Biomaterials Congress", 29 May–2 June, 1996, Toronto, Canada, p. 192.
  20. A. BELLARE and M. SPECTOR, in "24th Annual Meeting of the Society for Biomaterials", 22–26 April, 1998, San Diego, California, p. 124.
  21. M. GOLDMAN, R. GRONSKY and L. PRUITT, *J. Mater. Sci.: Mater. Med.* **9** (1998) 207.
  22. J. R. WHITE and A. TURNBULL, *J. Mater. Sci.* **29** (1994) 584.
  23. S. M. KURTZ, C. M. RIMNAC and D. L. BARTEL, in "42nd Annual Meeting, Orthopaedics Research Society", 19–22 February, 1996, Atlanta, Georgia, p. 492.
  24. S. M. KURTZ, C. M. RIMNAC, L. S. and D. L. BARTEL, in "40th Annual Meeting, Orthopaedic Research Society", 21–24 February, 1994, New Orleans, Louisiana, p. 289.
  25. K.-Y. LEE and D. PIENKOWSKI, in "42nd Annual Meeting, Orthopaedic Research Society", 19–22 February, 1996, Atlanta, Georgia, p. 468.
  26. O. K. MURATOGLU, L. MOUNIB, B. MCGORY, C. R. BRADGON, M. JASTY and W. H. HARRIS, in "24th Annual Meeting of the Society for Biomaterials", 22–26 April, 1998, San Diego, CA, p. 95.
  27. F. J. BUCHANAN, B. SIM and S. DOWNES, *Plastics, Rubber Comp. Process. Appl.* **27** (1998) 148.

*Received 12 March 1999  
and accepted 24 August 1999*